

ChemComm

Functionalised cyclodextrin-based metal-organic frameworks

K. J. Hartlieb,^a A. W. Peters,^a T. C. Wang,^a P. Deria,^a
O. K. Farha,^a J. T. Hupp,^a J. F. Stoddart^{*a}

^a Department of Chemistry, Northwestern University, 2145 Sheridan Road, Evanston, IL 60208, USA.

Supporting Information

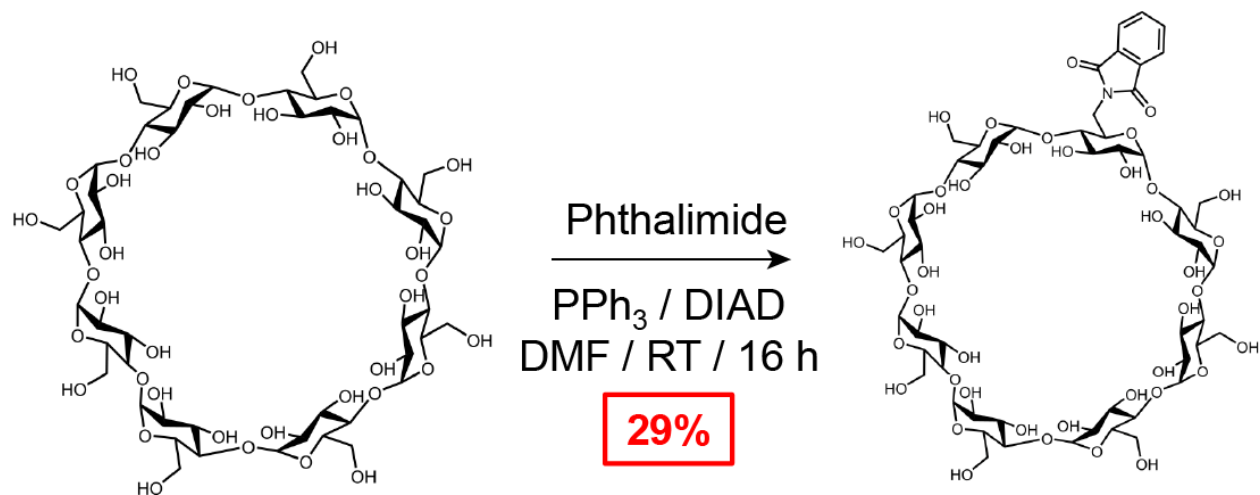
Table of Contents

S1. General Methods	S2
S2. Synthetic Procedures	S3
S3. Single Crystal X-Ray Crystallography	S6
S4. Powder X-Ray Crystallography	S8
S5. High Resolution Mass Spectrometry	S10
S6. ¹³C NMR Spectroscopy	S11
S7. BET Analysis	S12
S8. References	S13

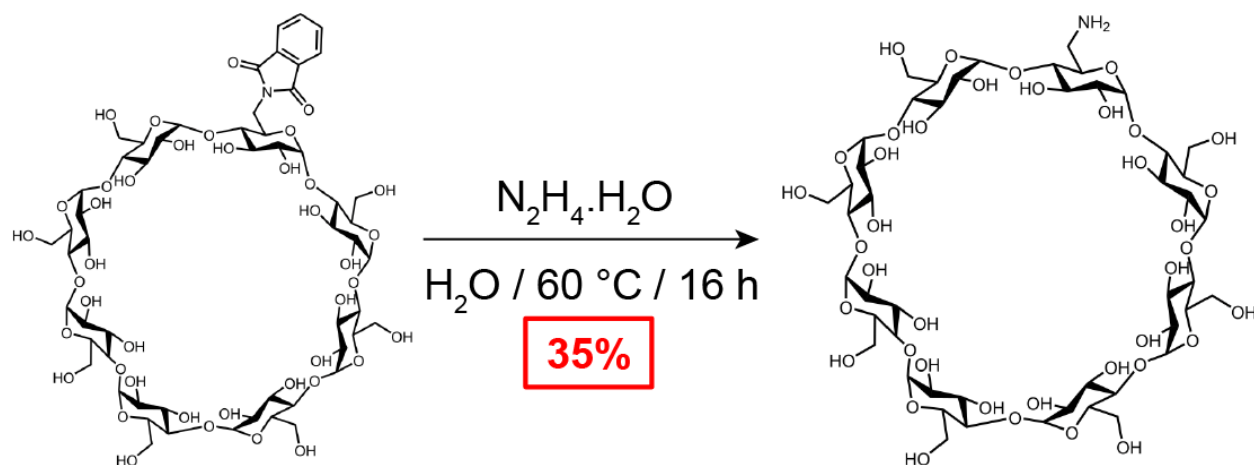
S1. General Methods

All reagents were purchased from commercial suppliers (Aldrich and AK Scientific) and used without further purification. Deuterated solvents (Cambridge Isotope Laboratories) for NMR spectroscopic analyses were used as received. Solution-state ^1H NMR spectra were recorded on Bruker Avance-500 spectrometers at 500 MHz at ambient temperature. All chemical shifts are quoted in ppm relative to the signals corresponding to the residual non-deuterated solvents (D_2O : $\delta_{\text{H}} = 4.79$ ppm, $(\text{CD}_3)_2\text{SO}$: $\delta_{\text{H}} = 2.50$ ppm). The following abbreviations are used to explain the multiplicities: s, singlet; d, doublet; t, triplet; m, multiplet or overlapping peaks. Preparative-scale High Performance Liquid Chromatography (HPLC) was carried out using an XBridge Prep C18 $5\mu\text{m}$ OBD column (19×100 mm) and the mobile phase consisted of Millipore H_2O and HPLC grade MeCN, both containing 0.1 % trifluoroacetic acid and separations were performed using a gradient of 0 \rightarrow 100% MeCN over 35 mins. Powder X-ray diffraction was performed on a Rigaku Miniflex 600 diffractometer operated at 40 kV using Cu $\text{K}\alpha$ radiation ($\lambda = 1.5418 \text{ \AA}$). Diffuse reflectance infrared Fourier transform spectra (DRIFTS) were recorded on a Nicolet iS 50 FT-IR spectrometer (Thermo Scientific) equipped with an MCT detector and a Harrick Praying Mantis accessory. The spectra were collected in a KBr mixture under Ar (ultrahigh purity) and CO_2 (research grade) diluted in Ar (final concentration $\sim 2\%$ CO_2), and KBr was utilised as the background. All samples were heated to 50°C under a flow of Ar (120 sccm) for 2 h before IR measurements were collected. Spectra were averaged over 64 scans with 1 cm^{-1} resolution. Nitrogen isotherms were measured on a Micromeritics TriStar II 3020 at 77 K and BET surface area analyses were consistent with the criteria described by Rouquerol^{S1} and Walton^{S2}. Preceding isotherm measurements, samples were heated to 50°C under vacuum for 12 h on a Micromeritics Smart VacPrep.

S2. Synthetic Procedures



6^A-Deoxy-6^A-phthalimido- γ -cyclodextrin 1: γ -CD (6.6 g, 5.1 mmol), dried under high vacuum at 130 °C overnight, phthalimide (0.9 g, 6.1 mmol) and PPh_3 (3.2 g, 12.2 mmol) were dissolved in anhydrous DMF (150 mL), followed by slow addition of diisopropyl azodicarboxylate (DIAD) (1.8 mL, 6.1 mmol) and the solution was stirred at ambient temperature overnight. The solvent was removed *in vacuo* and Me_2CO (200 mL) was added to the residue, followed by stirring for 1 h and filtration. The residue was dissolved in a 50 vol% $\text{H}_2\text{O}/\text{DMF}$ mixture and subjected to reverse-phase HPLC to give **1** as a white solid (2.1 g, 29 %). ^1H NMR (500 MHz, $(\text{CD}_3)_2\text{SO} / \text{D}_2\text{O}$ 80 / 20, 298 K, Referenced to $(\text{CD}_3)_2\text{SO}$) δ = 7.80 (s, 4H), 5.01 (m, 1H), 4.88 (m, 5H), 4.72 (m, 2H), 3.99 (d, J = 12.9 Hz, 1H), 3.90 (t, J = 10.4 Hz, 1H), 3.79 (m, 1H), 3.74 – 3.15 (m, 44H), 2.99 (m, 2H) ppm. ^{13}C NMR (125 MHz, $(\text{CD}_3)_2\text{SO} / \text{D}_2\text{O}$ 80 / 20, 298 K, Referenced to $(\text{CD}_3)_2\text{SO}$) δ = 169.4, 160.7, 160.5, 135.8, 132.2, 124.1, 103.2, 102.8, 102.7, 102.6, 101.5, 84.7, 81.8, 81.7, 80.4, 74.2, 73.9, 73.8, 73.7, 73.4, 73.3, 73.2, 73.1, 73.0, 72.9, 72.7, 72.6, 69.2, 61.1, 61.0, 60.8, 60.7, 60.6, 60.5, 59.3, 59.3, 40.1 ppm. HRMS: (m/z): calcd for $[M + \text{Na}]^+$: 1448.4336; found 1448.4338.



6^A-Deoxy-6^A-amino- γ -cyclodextrin **2:** $\text{N}_2\text{H}_4 \cdot \text{H}_2\text{O}$ (64 – 65%, 0.5 mL, 6.6 mmol) was added to a suspension of **CD 1** (300 mg, 0.2 mmol) in H_2O (15 mL) and the mixture was stirred while heated to 60 °C overnight. Me_2CO (100 mL) was then added to the solution in order to precipitate the crude product. The solid was recovered by centrifugation and was dissolved in the minimum quantity of H_2O and precipitated by addition of Me_2CO . This processes was repeated three times in order to yield pure **2** as a white solid (97 mg, 35 %). ^1H NMR (500 MHz, D_2O , 298 K) δ = 5.18 (d, J = 3.7 Hz, 1H), 5.13 (q, J = 4.0 Hz, 7H), 4.13 – 3.76 (m, 38H), 3.75 – 3.56 (m, 18H), 3.52 (t, J = 9.4 Hz, 1H), 3.43 (dd, J = 13.5, 3.0 Hz, 1H), 3.16 (dd, J = 13.6, 8.1 Hz, 1H). ppm. ^{13}C NMR (125 MHz, D_2O , 298 K), δ = 101.9, 101.8, 101.7, 82.3, 80.6, 80.5, 73.0, 72.5, 72.1, 71.7, 60.2, 41.3 ppm. HRMS: (m/z): calcd for $[M + \text{H}]^+$: 1296.4464; found 1296.4463.

NH_2 -CD-MOF-2**:** Although this framework can be prepared starting from either **1** or **2**, the framework generated using **1** contains phthalate anions within the pores of the framework, giving rise to a negative N_2 isotherm consistent with very low N_2 uptake. *Method 1:* **1** (50 mg, 0.035 mmol) and RbOH (29 mg, 0.28 mmol) were dissolved in H_2O (1 mL) and the resulting solution was divided into equal volumes in four crystallisation tubes. The solutions were exposed to

Me₂CO vapor for one week, after which time the resulting crystals were analysed by single-crystal X-ray crystallography and ¹H NMR spectroscopy (Fig. S1). *Method 2:* **2** (562 mg, 0.43 mmol) and RbOH (350 mg, 3.4 mmol) were dissolved in H₂O (10 mL) and the solution was divided into equal volumes in four crystallisation tubes. The solutions were exposed to MeOH vapor for two weeks, after which time they were washed with MeOH (5 × 20 mL) and dried under high vacuum overnight, giving 400 mg (61%) of an off-white crystalline powder. Powder X-ray diffraction confirms that this material crystallises in the same manner as that of CD-MOF-2 in the *I432* space group. Elemental analysis (%) calcd for [(C₄₈H₈₁O₃₉N)(RbOH)₂(H₂O)₈]_n: C 35.4, H 6.02, N 0.85; found: C 34.9, H 6.16, N 0.91 %.

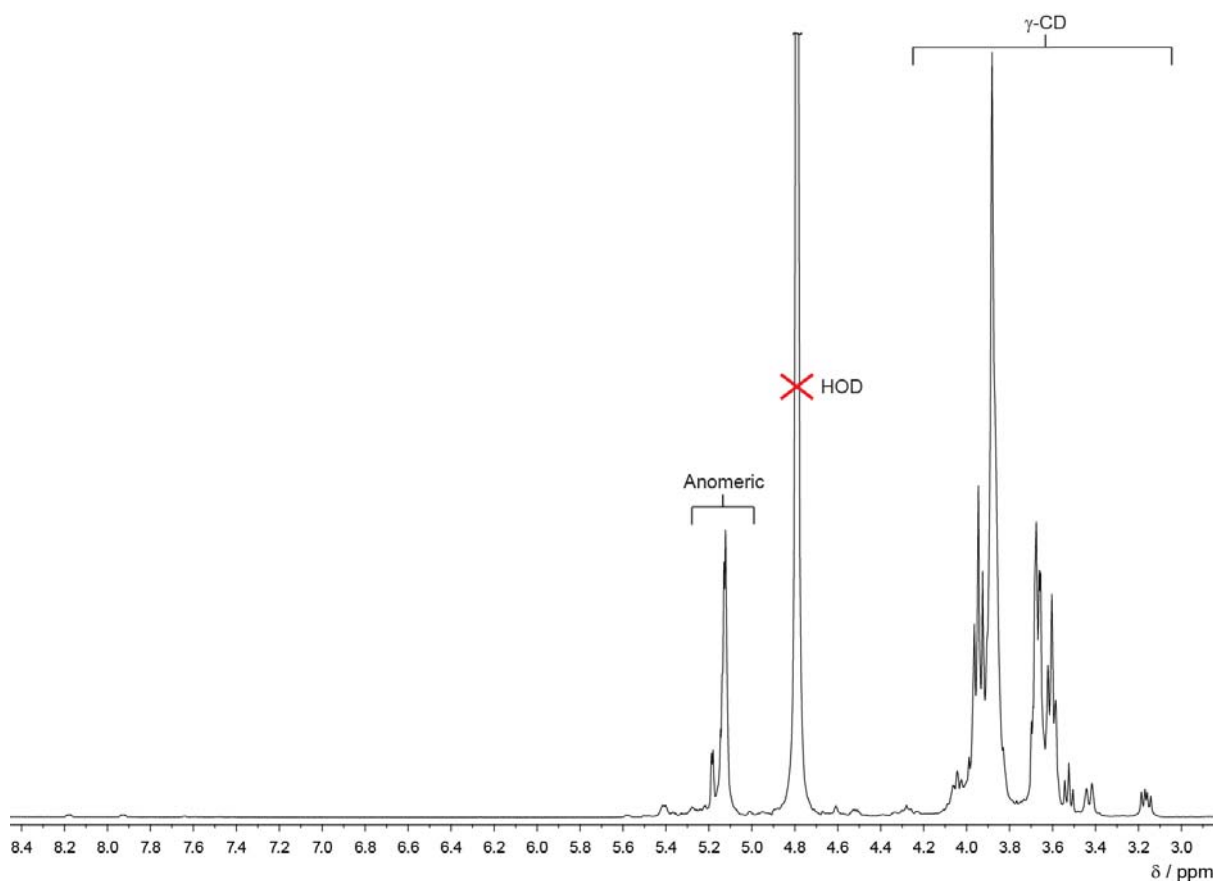


Fig. S1. ¹H NMR spectrum (500 MHz, D₂O, 298 K) of **2**. Very small signals present at ~ 8.2 and 7.9 ppm signify a trace quantity of phthalate present in the sample.

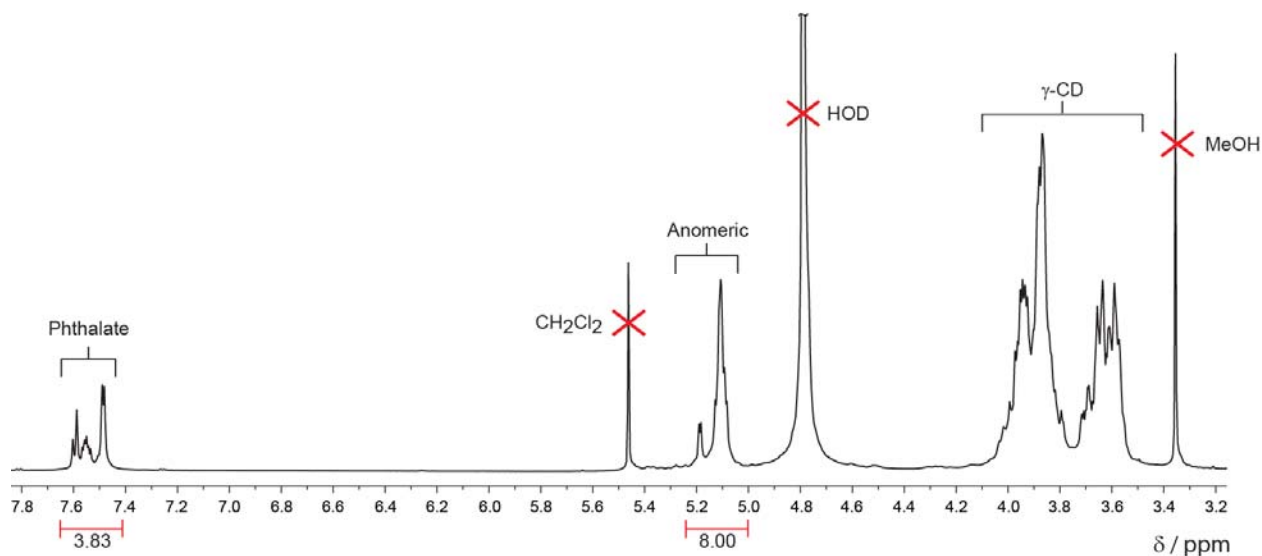


Fig. S2. ^1H NMR spectrum (500 MHz, D_2O , 298 K) of $\text{NH}_2\text{-CD-MOF-2}$ prepared from **1**. The phthalate anions are present in the framework in an approximately 2:1 ratio with respect to the γ -cyclodextrin.

S3. Single-Crystal X-Ray Crystallography

1: Single crystals suitable for X-ray analysis were grown by precipitation of **1** in D_2O . *Crystal data*: $\text{C}_{56}\text{H}_{83}\text{NO}_{41}$, $2(\text{H}_2\text{O})$; $M = 1462.26$ g/mol, orthorhombic, space group $P2_12_12_1$, $a = 11.9905(8)$, $b = 16.4042(11)$, $c = 37.700(3)$ Å, $V = 7415.3(9)$ Å³, $Z = 4$, $T = 99.91$ K, $\mu(\text{CuK}\alpha) = 0.989$ mm⁻¹, $D_{\text{calc}} = 1.310$ g/mm³, $\text{Flack} = -0.1(2)$, 60413 reflections measured ($7.144 \leq 2\Theta \leq 136.622$), 13418 unique ($R_{\text{int}} = 0.0543$, $R_{\text{sigma}} = 0.0455$) which were used in all calculations. The final R_1 was 0.0820 ($I > 2\sigma(I)$) and wR_2 was 0.2397 (all data). The solvent masking procedure as implemented in Olex2^{S3} was used to remove the electronic contribution of solvent molecules from the refinement. Total solvent accessible volume / cell = 1432.9 Å³ [19.3%] Total electron count / cell = 280.2. Crystallographic data for this structure have been deposited with the Cambridge Crystallographic Data Center as supplementary publication CCDC – 1525791.

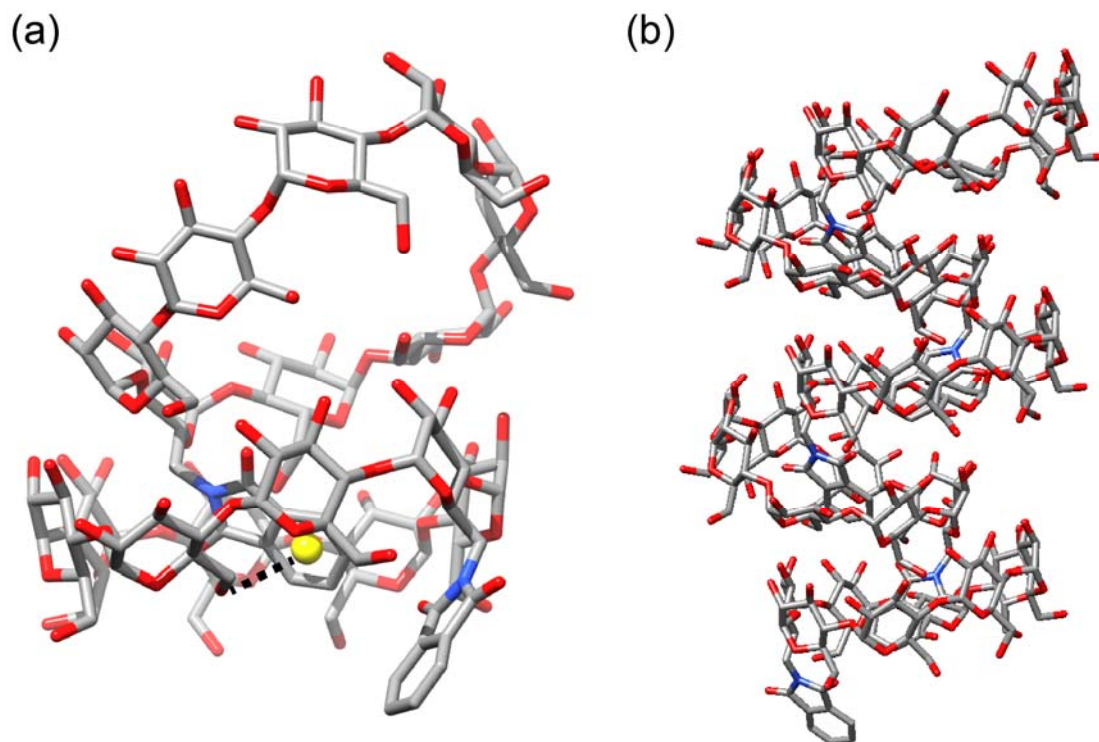


Fig. S3. Single crystal structure (grey: C, red: O, blue: N) of (a) a dimer of **1** with the dashed line representing the weak $[\text{OH}\cdots\pi]$ interaction (3.4 Å). The yellow sphere denotes the centroid of the aromatic ring of phthalimide. (b) 1D Chain of **1** formed by supramolecular interactions of the phthalimide units with the γ -CD tori.

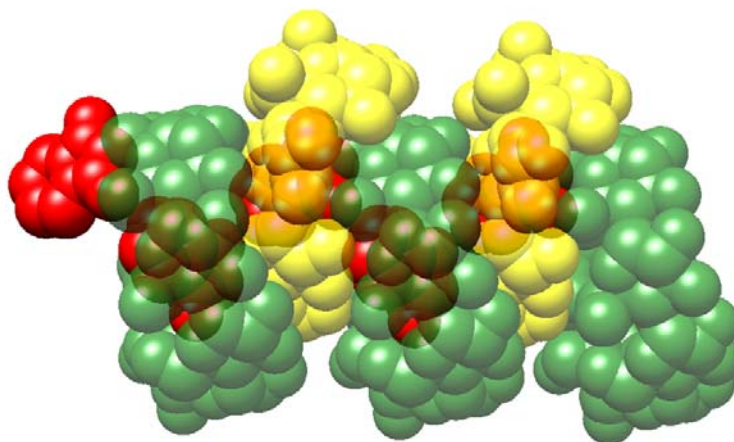


Fig. S4. Space-filling representation of the solid-state supramolecular polymer of **1**. Phthalimide units are shown in red, while the γ -CD units having two different orientations are shown in green and yellow.

NH₂-CD-MOF-2: *Crystal data:* C₄₈H₈₁NO₃₉Rb₂; $M = 1467.07$ g/mol, cubic, space group *I432*, $a = 31.0197(11)$ Å, $V = 29848(3)$ Å³, $Z = 12$, $T = 100.0$ K, $\mu(\text{CuK}\alpha) = 1.849$ mm⁻¹, $D_{\text{calc}} = 0.979$ g/mm³, $\text{Flack} = 0.017(10)$, 228205 reflections measured ($4.028 \leq 2\Theta \leq 136.62$), 4595 unique ($R_{\text{int}} = 0.0546$, $R_{\text{sigma}} = 0.0130$) which were used in all calculations. The final R_1 was 0.0586 ($I > 2\sigma(I)$) and wR_2 was 0.2040 (all data). The solvent masking procedure as implemented in Olex2^{S3} was used to remove the electronic contribution of solvent molecules from the refinement. Total solvent accessible volume / cell = 12922.3 Å³ [43.3%] Total electron count / cell = 4098.5. *Refinement details:* Through synthetic methods it is known that there is only one amine per CD ring. Therefore, the occupancies of N1 and N1A were refined to sum to 0.25. The occupancies of the corresponding OH groups were restrained to sum to 1 minus the occupancy of the corresponding amine. C-O and C-N distances of these disordered groups were refined with similarity restraints (SADI) and a group anisotropic displacement parameter was used for the O and N atoms. Crystallographic data for this structure have been deposited with the Cambridge Crystallographic Data Center as supplementary publication CCDC – 1525790.

S4. Powder X-Ray Crystallography

Powder XRD patterns confirm the NH₂-CD-MOF-2 crystallised from both **1** and **2** form frameworks that crystallise in the *I432* space group, similar to that observed in the case of CD-MOF-2^{S4}

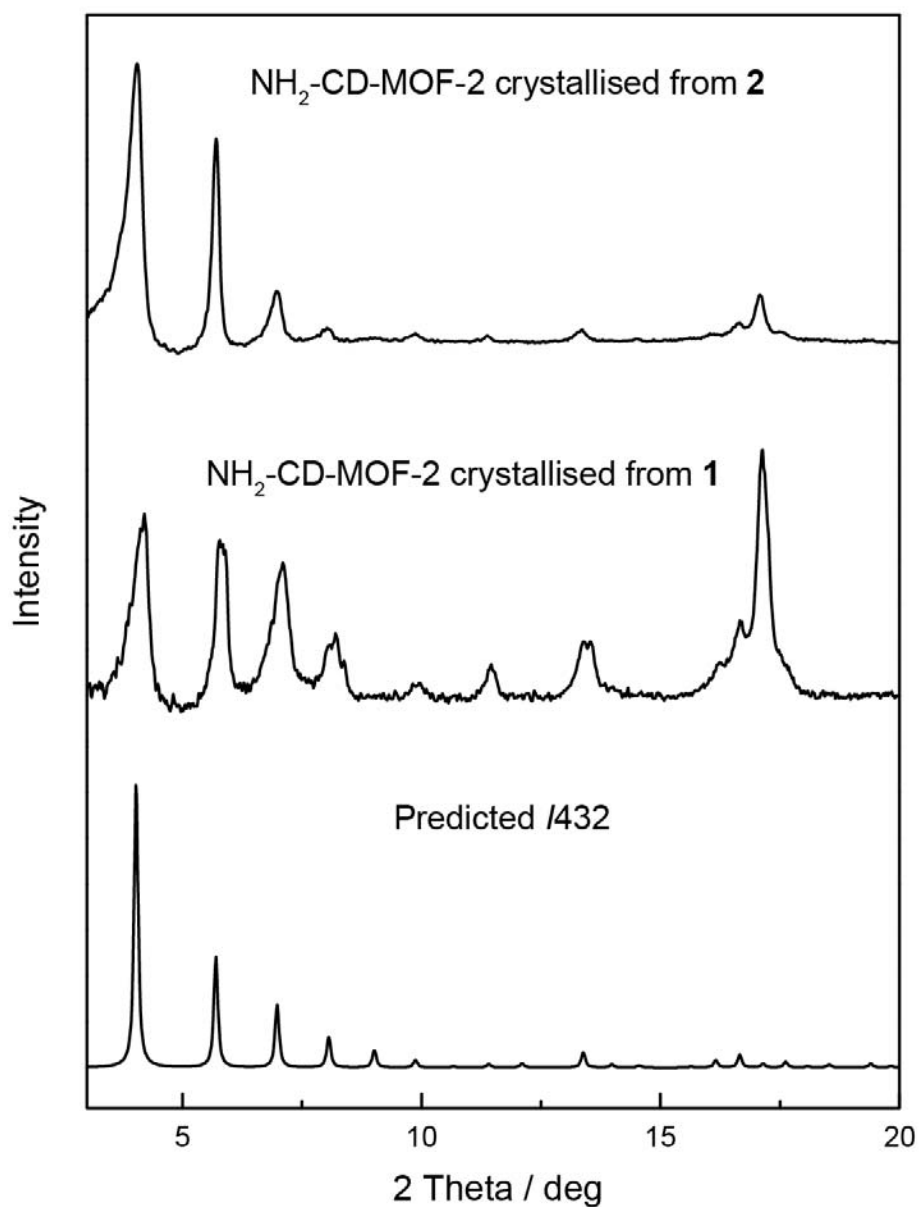


Fig. S5. PXRD patterns of NH₂-CD-MOF-2 crystallised from both **1** and **2** and a comparison to the predicted *I432* pattern from CD-MOF-2.

S5. High Resolution Mass Spectrometry

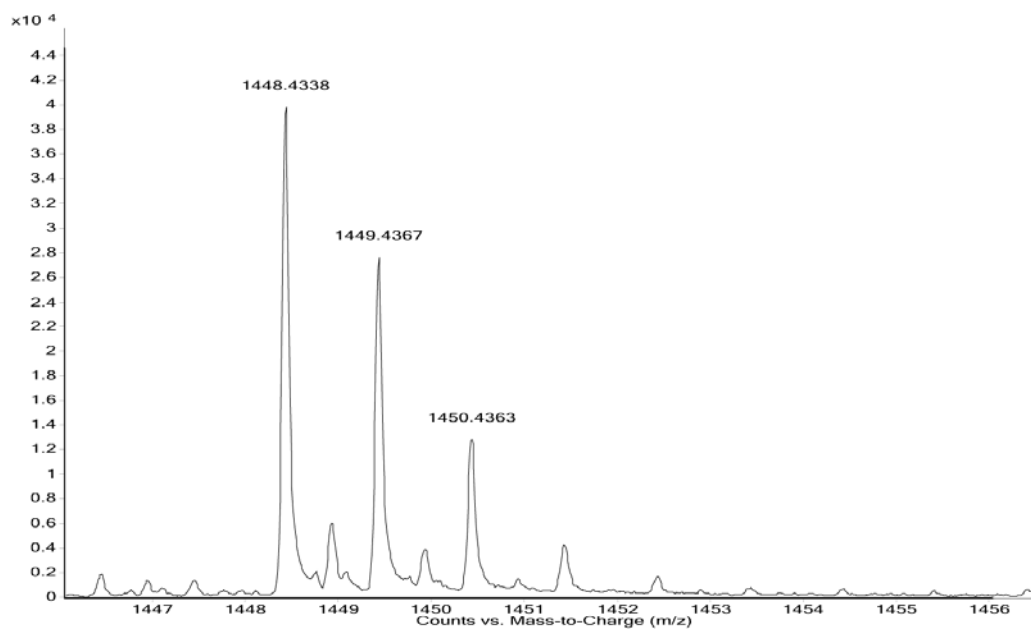


Fig. S6. High resolution spectrum of **1** showing the $[M + \text{Na}]^+$ signal at $m/z = 1448.4338$.

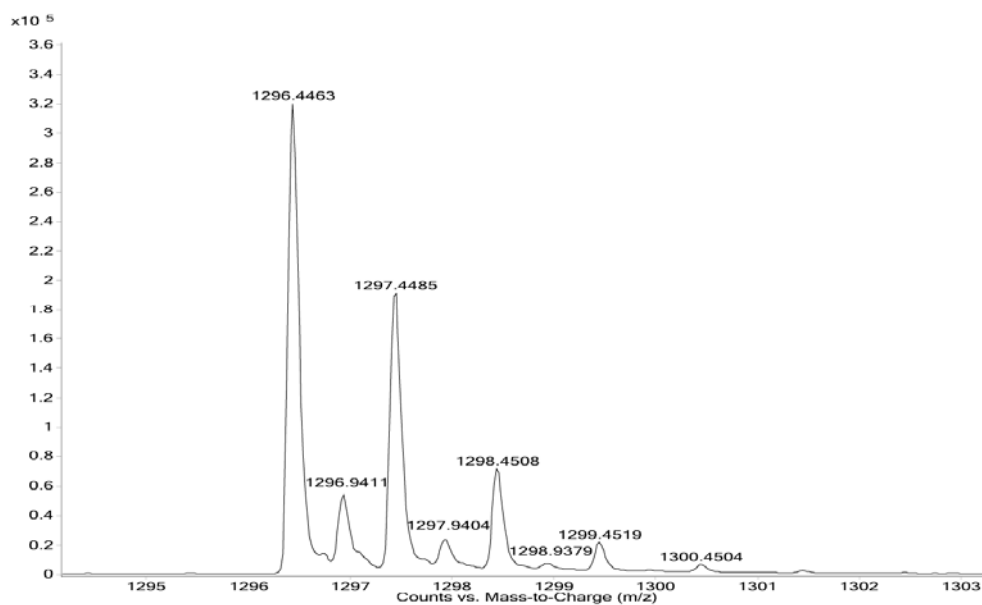


Fig. S7. High resolution spectrum of **2** showing the $[M + \text{H}]^+$ signal at $m/z = 1296.4463$.

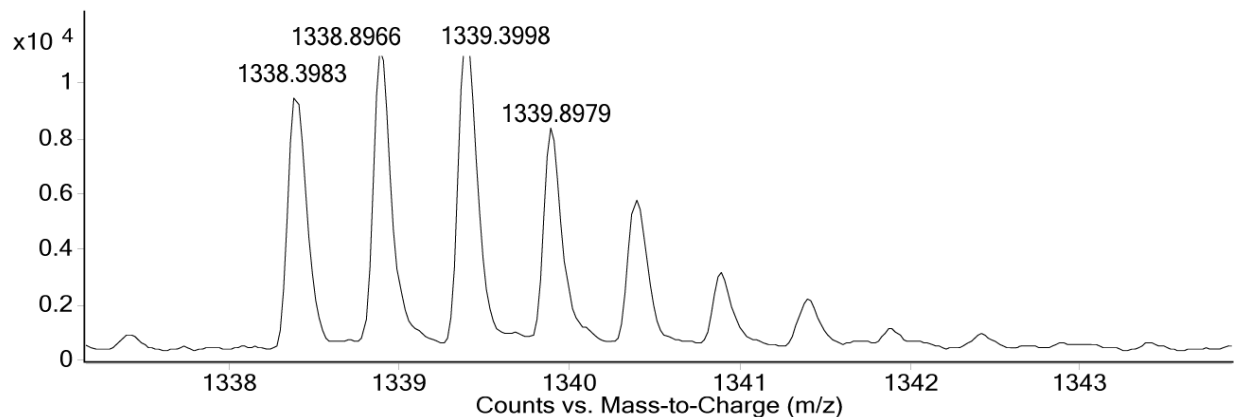


Fig. S8. High resolution spectrum of **NH₂-CD-MOF-2** after exposure to CO₂ showing the $[2M + H + Rb]^{2+}$ signal at $m/z = 1338.3983$.

S6. ¹³C NMR Spectroscopy

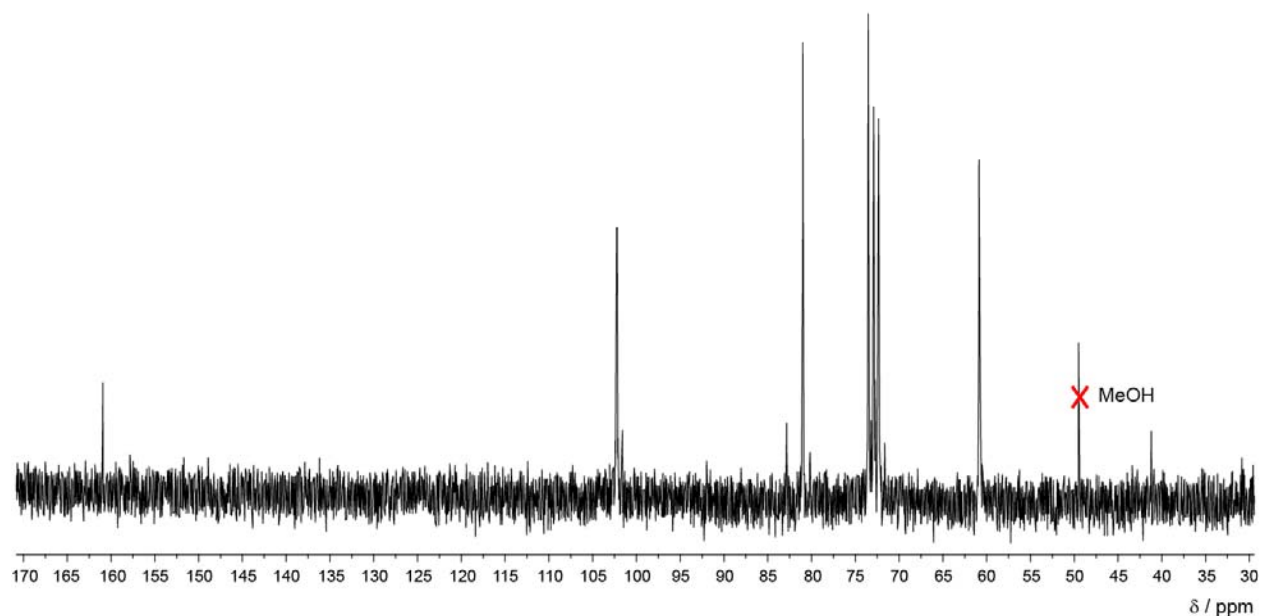


Fig. S9. ¹³C NMR (125 MHz, 298 K, D₂O) spectrum of **NH₂-CD-MOF-2** after exposure to CO₂ revealing a signal at ~160 ppm which may be a result of the presence of bicarbonate in solution after hydrolysis of the carbamic acid group generated upon exposure of the MOF to CO₂.

S7. BET Analysis.

The consistency criteria described by Rouquerol et al.^{S1} and Gómez-Gualdrón et al.^{S6} are considered and met for the presented Brunauer–Emmett–Teller (BET) analysis.

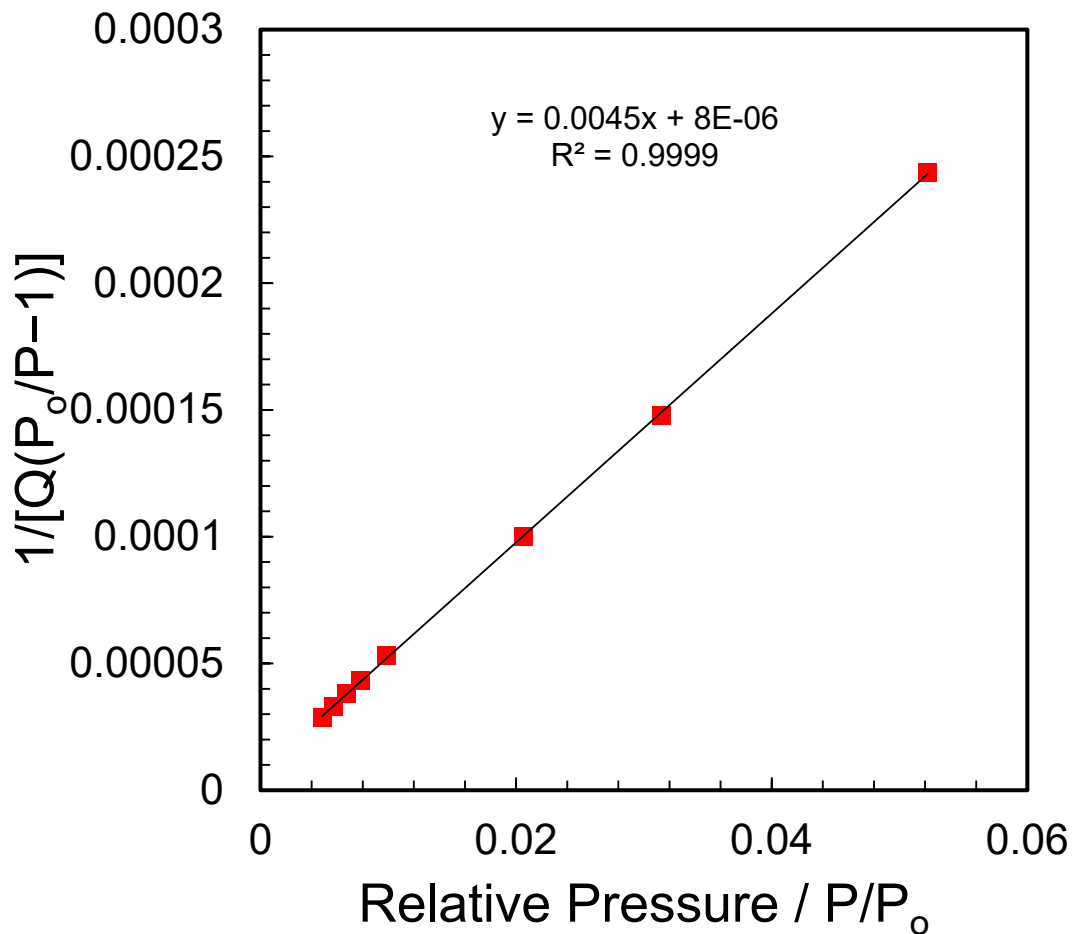


Figure S10. BET plot of NH₂-CD-MOF-2 corresponding to the N₂ isotherm shown in the inset of Figure 3.

Table S1. BET parameters from the experimental N₂ isotherm at 77 K of NH₂-CD-MOF-2

BET Area (m ² /g)	Slope	Y-intercept	R ²	C, BET Constant	n _m (cm ³ /g)	P/P ₀ at n _m
963 ± 4	0.00415	8.00 x 10 ⁻⁶	1.00	601	221	0.0314

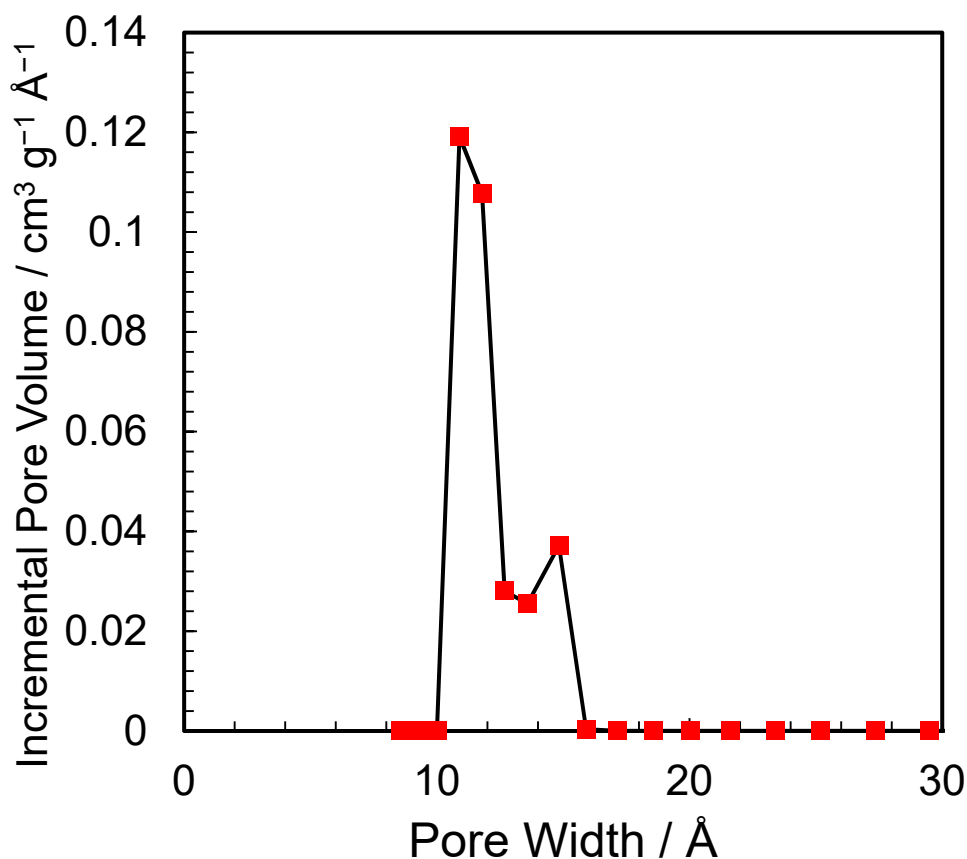


Figure S11. DFT pore size distribution of NH₂-CD-MOF-2 using a carbon slit pore model with an N₂ DFT kernel.

S8. References.

- S1. J. Rouquerol, P. Llewellyn, F. Rouquerol, *Stud. Surf. Sci. Catal.* 2007, **160**, 49.
- S2. K. S. Walton, R. Q. Snurr, *J. Am. Chem. Soc.* 2007, **129**, 8552.
- S3. O.V. Dolomanov, L.J. Bourhis, R. J. Gildea, J.A.K. Howard, H. Puschmann, *J. Appl. Cryst.*, 2009, **42**, 339.
- S4. R. S. Forgan, R. A. Smaldone, J. J. Gassensmith, H. Furukawa, D. B. Cordes, Q. Li, C. E. Wilmer, J. M. Spruell, Y. Y. Botros, R. Q. Snurr, A. M. Z. Slawin, J. F. Stoddart, *J. Am. Chem. Soc.*, 2012, **134**, 406.
- S6. D. A. Gómez-Gualdrón, P. Z. Moghadam, J. T. Hupp, O. K. Farha, R. Q. Snurr, *J. Am. Chem. Soc.*, 2016, **138**, 215.